LA-UR-02-3575

Approved for public release; distribution is unlimited.

Title: FRAGMENTATION RESPONSE OF AGED MILLIWATT FUEL

Author(s): Jonathan G. Teague
Mary Ann Reimus
Art R. Herrera
Paul F. Moniz

Submitted to: DOE-NE50

Los Alamos
NATIONAL LABORATORY

Form 836 (8/00)

TABLE OF CONTENTS

LIST OF TABLES

LIST OF FIGURES

FUEL FRAGMENTATION RESPONSE OF AGED MILLIWATT FUEL

Abstract

Four milliwatt heat sources were impacted side-on against steel at 30, 40, 50, and 60 m/s respectively using the Isotopic Fuels Impact Tester (IFIT) 7" launcher at the TA-55 Plutonium Facility. Particle size analyses were performed on the recovered fuel from each capsule to determine the fragmentation response of aged fuel. Particle size data obtained from two un-impacted milliwatt capsules were compared to historical un-impacted particle size data to evaluate the effect of aging alone on fuel particle fragmentation. Fuel particle size data from two un-impacted milliwatt capsules were then compared to the impacted capsules to determine any differences between fuel fragmentation response due to aging alone, and fragmentation response due to aging and impact. Limited particle size data show that the effect of long-term aging alone on fuel particle fragmentation is small. There does appear to be a correlation between impact velocity/ capsule deformation and the generation of fines in the < 10-micron size range. Nevertheless, fuel fragmentation response of the impacted capsules was not substantially different from the non-impacted capsules.

INTRODUCTION

Knowledge of the fuel fragmentation response of a plutonia fueled heat source resulting from impact is essential for establishing a respirable source term should capsules fail under accident conditions. Furthermore, fuel aging can result in the generation of additional respirable fuel particles during the course of the heat source lifetime. In this work, we have examined milliwatt heat sources, which have been in service since the late 1970's, to study the effects of long-term aging on fuel particle fragmentation. We also looked at the effect of impact on fuel particle fragmentation. Milliwatt capsules were fueled with Pu-238 oxide granules fired at 1600°C for 6 hours and then screened such that the particle size range was 53-500 μm[1-5]. After the fuel was loaded into the strength member, the fuel was reduced from PuO_2 to $PuO_{1.75}$ by heating in a vacuum furnace at 1350°C. Possible lattice vacancies in the microstructure of $PuO_{1.75}$ could cause a different fuel fragmentation response than stoichiometric $PuO_{2.0.}$ For a complete milliwatt fuel processing flow diagram see appendix A.

Four milliwatt heat sources, all fueled in 1978, were recovered from their respective RTG and individually impact tested at velocities ranging from 30 to 60 m/s in the IFIT. A sketch of the milliwatt heat source capsule is shown in appendix B. Particle size distribution analyses were performed on the fuel recovered from each of the impacted capsules to determine the extent of fuel particle fragmentation. Particle size distribution analyses were also performed on fuel recovered from two non-impacted capsules, also fueled in 1978. Non-impact particle size distribution data were compared to historical non-impact data to determine the effect of long-term aging on fuel particle fragmentation. Particle size distributions from the four impacted heat sources were also compared to the un-impacted distributions to illustrate the change in fuel particle fragmentation response due to impact.

TEST SETUP

Individual milliwatt capsules were impacted side-on against a steel target in the IFIT 7" launcher located in PF-4 at TA-55. A sketch of the IFIT is provided in Figure 1.

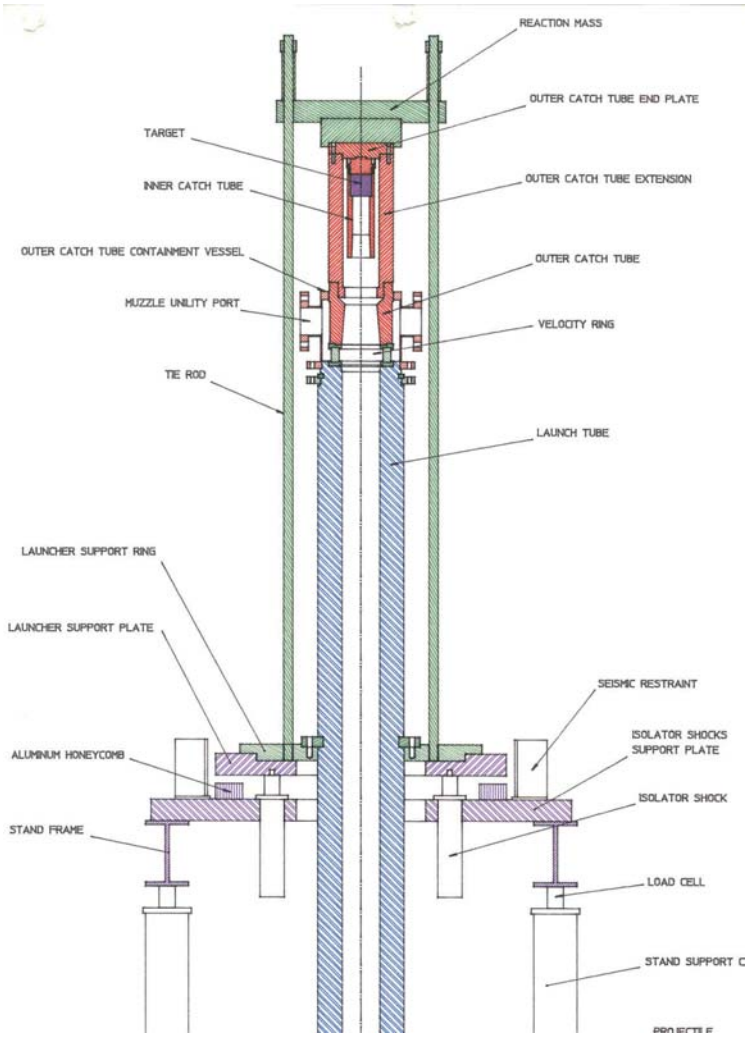

Figure 1. IFIT Assembly Schematic

The IFIT is a gas-driven device with a 178-mm (7-in) bore used for impacting $^{238}PuO_2$ heat sources at various temperatures. The IFIT was used to accelerate individual milliwatt heat sources that were heated by a resistance furnace built into the projectile. Dual containment of the heat source was achieved by using two vessels that are sealed directly to the barrel of the launcher. The heat source and associated furnace assembly sits on the inner projectile cylinder or IPC. The IPC in turn sits on the outer projectile cylinder or OPC. When the launcher is fired, this assembly travels towards the target.

The OPC is swaged into the outer catch tube or OCT providing the primary seal. The IPC carrying the heat source and furnace continue towards the target until the IPC is swaged into the inner catch tube or ICT. The heat source then continues on to the target. After impact, each milliwatt heat source was introduced into the glovebox line and recovered from the ICT for particle size analysis. A typical milliwatt projectile assembly with resistive element heater is shown in Figure 2.

Figure 2. A typical projectile assembly

The outer projectile cylinders for 30 and 40 m/s impacts were fabricated from brass to achieve the lower velocities. The 50 and 60 m/s impacts were performed using aluminum outer projectiles. Projectile velocity was measured by recording the time that a series of signal wires was severed by the projectile as it traveled towards the target. Capsule temperature was estimated by placing a thermocouple in close proximity to the heat source.

After an impact test, the sealed catch tube containing the heat source was transferred to the glovebox line and opened. The test components were removed and photographed. Post-impact dimensional measurements were made of each impacted heat source. The fuel granules were recovered by drilling a hole into the domed end of the heat source and pouring the fuel into a fuel container. Fuel granules recovered after impact were sieved on 3-inch certified sieves down to the 45-micron size range. Particle size characterization of fuel particles less than 45-microns was performed using a Galai WCIS-100 particle size analyzer. Raw data from the particle size analyzer were then transferred via RS232 interface to a desktop computer for tabulation.

RESULTS AND DISCUSSION

Aged Fuel Fragmentation Response

The particle size data from the two non-impacted heat sources is shown in Table 1. The weight fraction of fuel particles < 125 microns in size was greater for 619-F78 than for 437-D78. The weight fraction of 619-F78 § 10 microns was approximately 0.020 weight percent greater than for 437-D78. Figure 3 is a graphical comparison plot of the particle size distribution of the two non-impacted heat sources.

Table 1 Non-impacted heat source particle size distribution by weight fraction

Particle Size (micron)	619-F78 Non-Impact	437-D78 Non-Impact
+425 to 850	0.0143	0.0098
+180 to 425	0.1865	0.5272
+125 to 180	0.0875	0.1166
+75 to 125	0.1361	0.1133
+45 to 75	0.3649	0.1457
+30 to 45	0.0491	0.0169
+20 to 30	0.0539	0.0196
+10 to 20	0.0702	0.0336
+9 to 10	0.0044	0.0024
+8 to 9	0.0027	0.0018
+7 to 8	0.0034	0.0016
+6 to 7	0.0021	0.0016
+5 to 6	0.0020	0.0018
+4 to 5	0.0027	0.0018
+3 to 4	0.0057	0.0023
+2 to 3	0.0045	0.0013
+1 to 2	0.0100	0.0027
<1	0.0000	0.0000

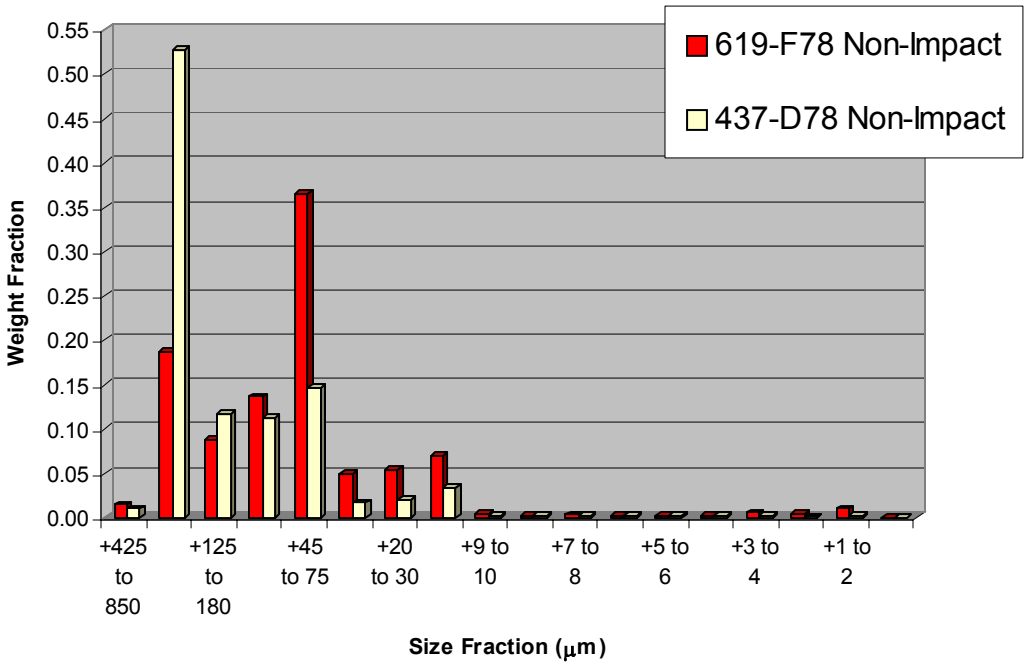

Figure 3. Non-Impact Particle Size Distribution Comparison

The particle size data from the 619-F78 and 437-D78 were compared to historical non-impact data obtained from surveillance milliwatt heat source manufactured from 1977 to 1978 and analyzed from 1982 to 1996. [1-5] The non-impact comparison data are shown in Table 2.

Table 2 Non-Impact Historical Comparisons

	Weight (g)				
	< 20	10 to 20	5 to 10	<5	Period Analyzed
619-F78	1.13	0.74	0.15	0.24	10/2001-12/2001
437-D78	0.47	0.31	0.08	0.07	10/2001-12/2001
0374-C78	0.53	0.20	0.19	0.14	4/83-3/84
0446-D78	0.46	0.20	0.12	0.14	4/83-3/84
0472-D78	0.50	0.21	0.16	0.13	4/83-3/84
0696-G78	0.10	0.05	0.02	0.03	4/83-3/84
0211-A78	0.17	0.05	0.10	0.02	4/84-3/86
0270-A78	0.13	0.06	0.04	0.03	4/84-3/86
0090-K77	0.56	0.28	0.16	0.12	4/86-3/88
1048-A79	0.22	0.06	0.09	0.07	4/86-3/88
0319-B78	0.17	0.11	0.04	0.02	4/88-9/96
0106-K77	0.07	0.03	0.03	0.01	4/82-3/83
0113-K77	0.06	0.03	0.02	0.01	4/82-3/83
0129-K77	0.28	0.11	0.11	0.06	4/82-3/83
0177-L77	0.38	0.16	0.16	0.06	4/82-3/83
0184-L77	0.33	0.14	0.14	0.05	4/82-3/83
0227-A78	0.17	0.07	0.06	0.04	4/82-3/83
Historical Average	0.28	0.12	0.10	0.06	
Historical 1 Standard Dev	0.17	0.08	0.06	0.05	

Fuel recovered from heat source 619-F78 had a different particle size distribution compared to other non-impact test specimens. On the other hand, the particle size distribution of fuel recovered from heat source 437-D78 was similar to the historical data. Figure 4 shows the non-impact data in bar graph form. The average and standard deviation of the historical data are presented in an attempt to understand the difference in fragmentation response between 619-F78 and the other particle size distribution data from a statistical standpoint.

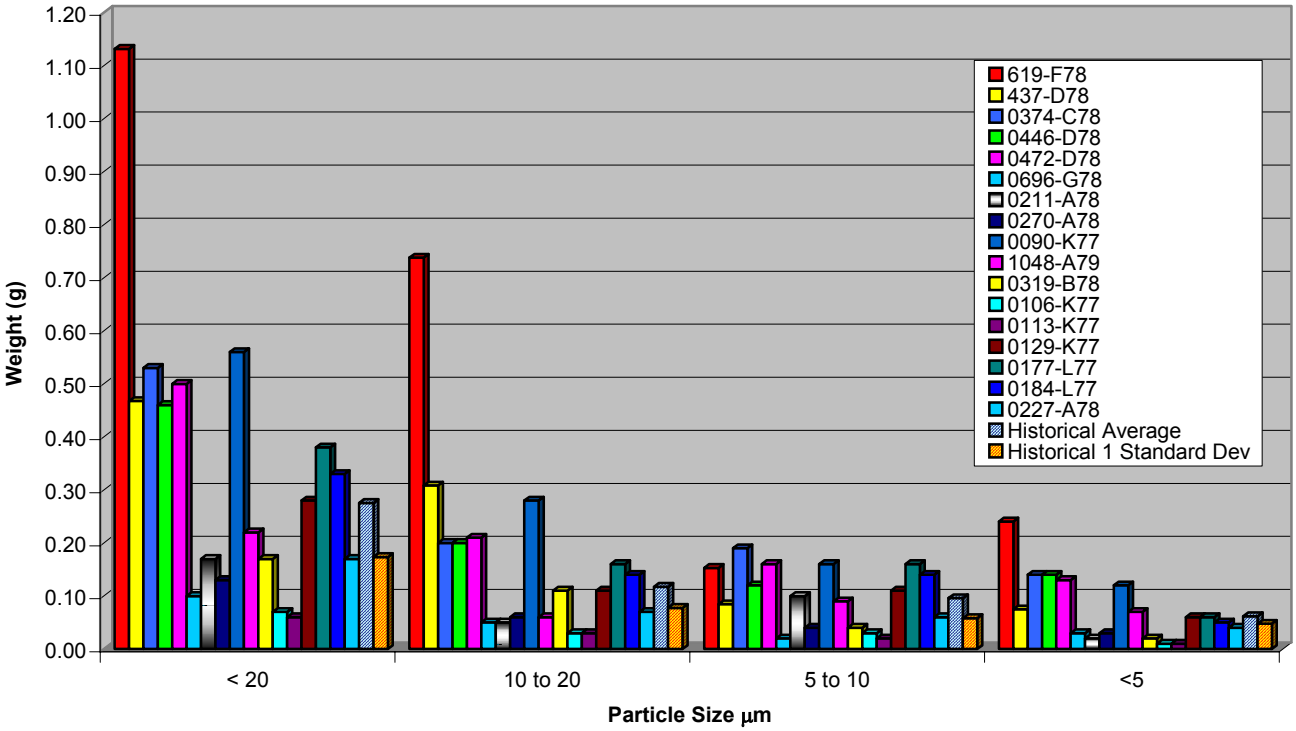

Figure 4. Non-Impact Historical Comparisons

It is evident that the fuel fragmentation of 619-F78 is different from both the other non-impacted heat source evaluated recently and all the other non-impacted heat sources for which particle size data are presented. Heat source 619-F78 is five standard deviations from the average at the < 20-micron size range, seven standard deviations from average at the 10-20 micron size range and about 3 standard deviations from the average at the < 5-micron size range. Conversely, the amount of fuel in the 5 to 10 micron size range of heat source 619-F78 is within 1 STD of average. The difference in particle size distribution between 619-F78 and the other non-impacted heat sources could be due in part to differences in operating environments, for example, but that cannot be verified. In contrast, fuel particle fragmentation response of heat source 437-D78 was very similar to the historical particle size data in all size ranges, indicating that fuel particle fragmentation due to aging alone may be small. However, a larger statistical sample would need to be evaluated to fully quantify the extent of aging alone on fuel particle fragmentation response.

Milliwatt Clad Impact Response

Four individual milliwatt capsules, heated to 350°C, were impacted side-on against a steel target at 30, 40, 50, and 60 m/s respectively. The fuel from each heat source was then recovered and the fuel particle size distribution measured. The fuel weights

recovered are presented in Table 3. The diametral strain of heat sources impacted at 50 and 60 m/s was measured and is listed in Table 4. Strain measurements were not performed on the other two impacted heat sources.

Table 3 Recovered Fuel Weights

619-F78	437-D78	0462-D78	0726-H78	0746-H78	0644-F78
Non-Impact	Non-Impact	30 m/s	40 m/s	50 m/s	60 m/s
10.51grams	9.18 grams	9.58 grams	10.34 grams	9.8 grams	10.24 grams

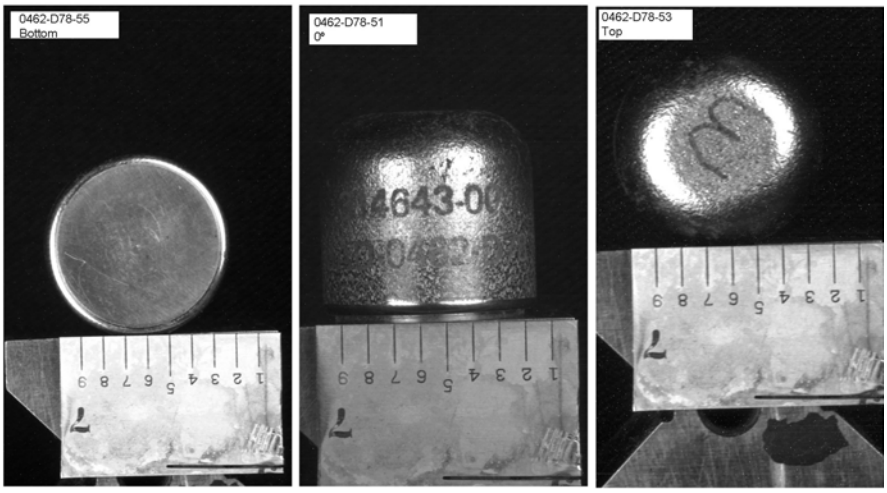

Figure 5. 462-D78 Pre-Impact

Capsule 462-D78 was impacted against a steel target at 30.04 ≤ 0.16 m/s. The temperature of the heat source at the time of firing was 355°C. The majority of the deformation due to impact occurred on the dome or top of the strength member at a small angle perpendicular to the cylindrical axis of the heat source, indicating that the heat source hit the target at an oblique angle (Figure 6). It is noted that the number three (3) observed in figure 5 is no longer visible after the impact in figure 6. This is likely a result of the impact event. The capsule did not breach.

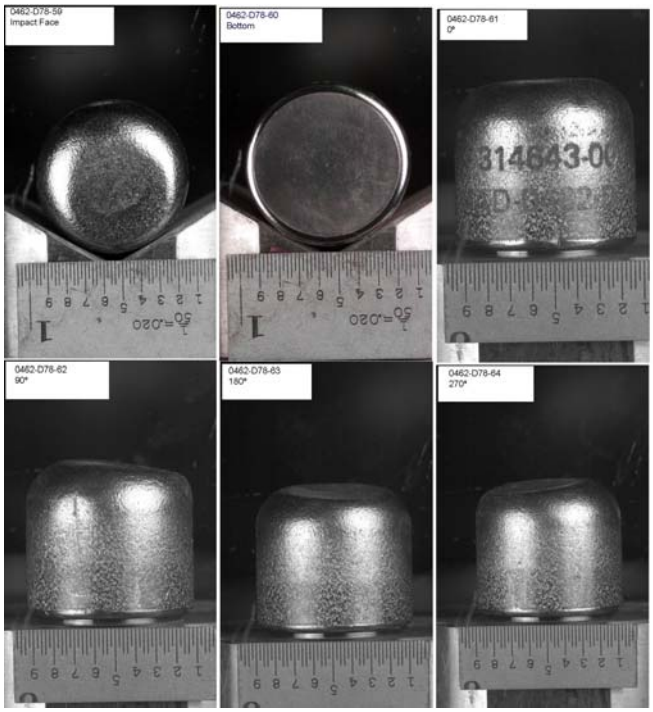

Figure 6. 462-D78 Post-Impact at 30 m/s

Capsule 726-H78 was impacted against a steel target side-on at 37.44 ≤ 0.35 m/s. The heat source temperature at the time of firing was 359°C. The majority of deformation occurred on the cylindrical region of the strength member with the largest plastic flow occurring at the base of the strength member at the interface between the domed member and the bottom cap (Figure 7). The capsule did not breach.

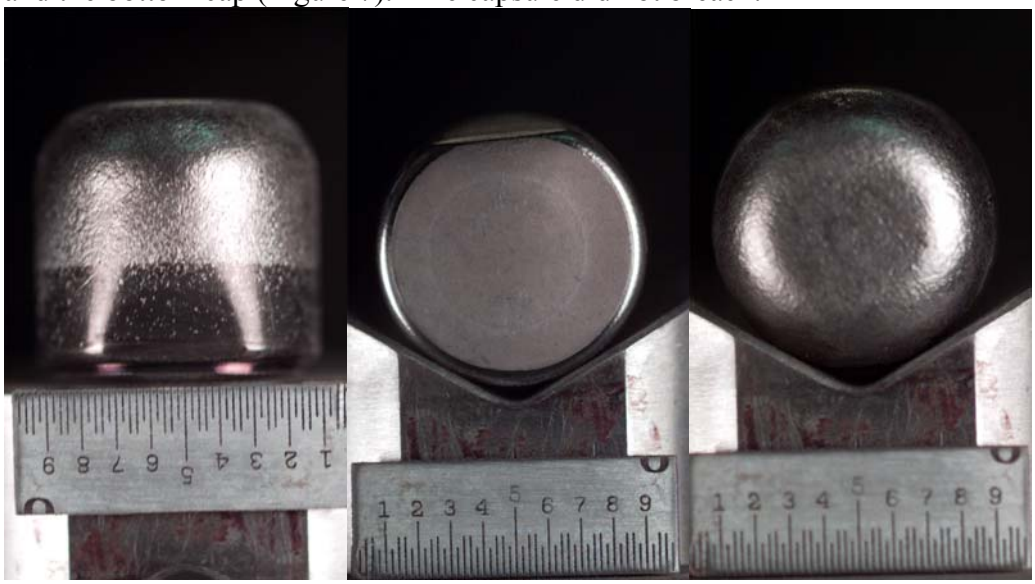

Figure 7. 726-H78 Post-Impact at 37 m/s

Capsule 746-H78 was impacted side-on against a steel target at 50.97 ≤ 0.12 m/s. The capsule temperature at the time of firing was 355°C. As expected, the deformation of capsule 746-H78 was greater than that observed for 726-H78. The plastic flow was more uniformly distributed across the impact face of the capsule (Figure 8). The maximum diametral strain of impacted heat source 746-H78 was approximately 1%. The minimum strain, or reduction in diameter, was approximately –2.5%. The capsule did not breach.

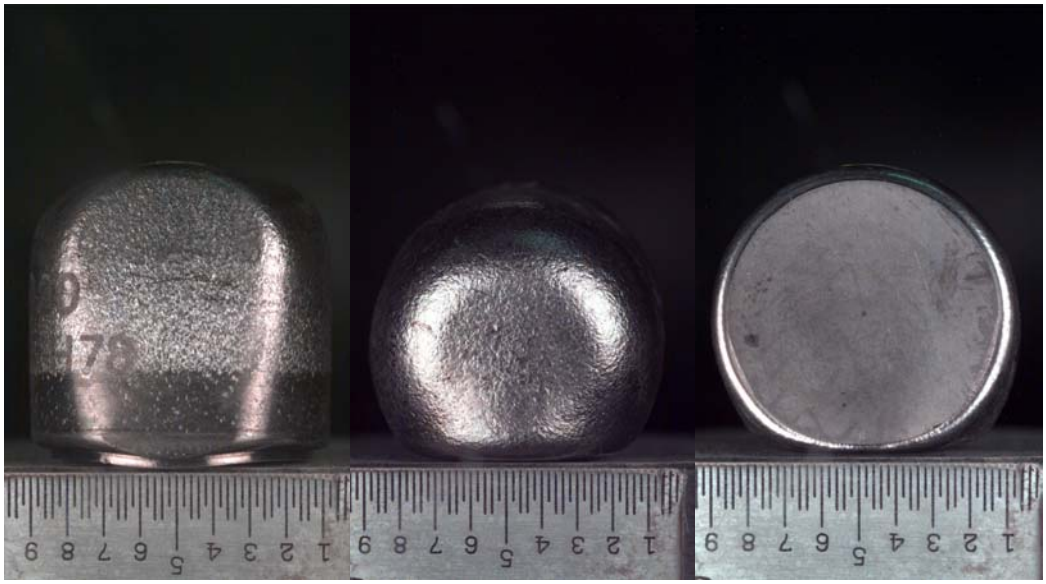

Figure 8. 746-H78 Post-Impact at 51 m/s

Capsule 644-F78 was impacted side-on against a steel target at 59.87 ≤ 0.18 m/s. The capsule temperature at the time of firing was 350°C. The maximum diametral strain, or increase in diameter, was 1.5% and the minimum strain or reduction in diameter was about –11% (Figure 9). The capsule did not breach.

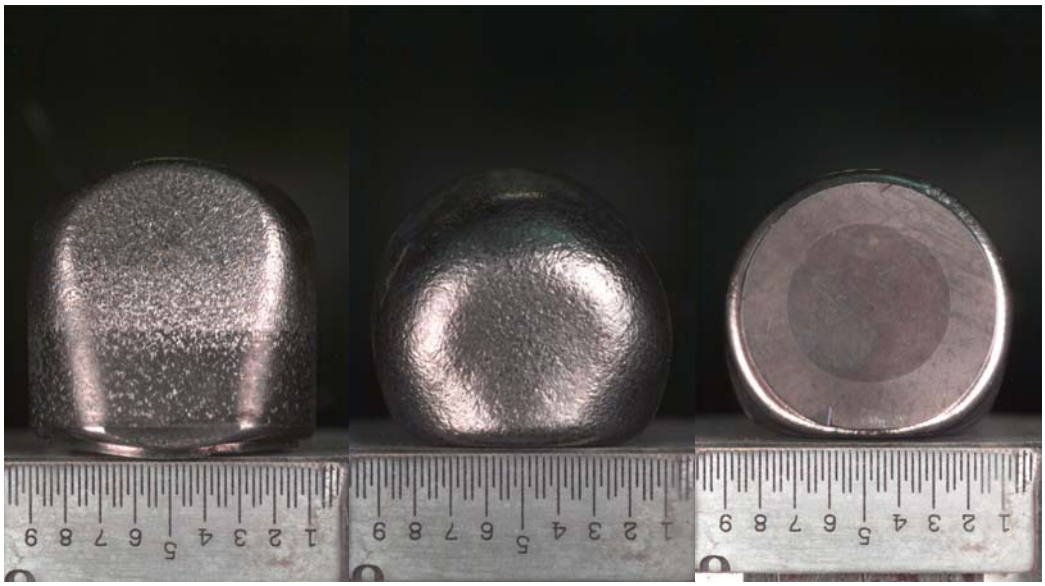

Figure 9. 644-F78 Post-Impact at 60 m/s

Table 4 shows a comparison of diametral strain between 746-H78 impacted at 50 m/s and 644-F78 impacted at 60 m/s. Strain data for the other two impacted heat sources were not available. The heat source impacted at 60 m/s experienced approximately four times the strain as the heat source impacted at 50 m/s. It is important to note that the strains experienced by the capsule impacted at 60 m/s were relatively low and no breach was observed, as expected for these velocities. The strain results are consistent with those expected due to increased impact energy. The kinetic energy of a moving object with constant mass increases as the square of the velocity; therefore, one would expect a

significant increase in the plastic deformation, or strain, for relatively small increases in velocity.

Table 4 Impacted Heat Source Diametral Strain

Nominal Diameter:		21.36 mm	
Clad	0644-F78	0746-H78	
Impact Velocity,	60	50	
(m/s)			
Max Dia.	21.68 mm	21.58 mm	
Min Dia.	19.04 mm	20.82 mm	
%Max Strain	1.50	1.03	
%Min Strain	-10.86	-2.53	

Particle size analysis was performed on all four impacted heat sources to determine the fuel fragmentation response at each impact velocity. Figure 10 is a graphical representation of the particle size distribution for each impacted heat source. Table 5 shows the particle size distribution data in tabular form. The particle size distribution for each impacted heat source shifted towards the smaller size fractions, as the impact velocity was increased. This behavior is expected, as the fuel absorbs more energy at the higher velocities resulting in fracture of fuel granules. A significant increase in the § 75 microns weight fraction occurs at velocities ¥ 50 m/s.

The particle size distributions from the impacted heat sources were also compared to the two non-impacted heat sources to illustrate the effect of impact on fuel particle fragmentation. Figure 11 show that the increase in fuel fragmentation of the impacted heat sources is very small compared to the fuel fragmentation of the non-impacted heat sources.

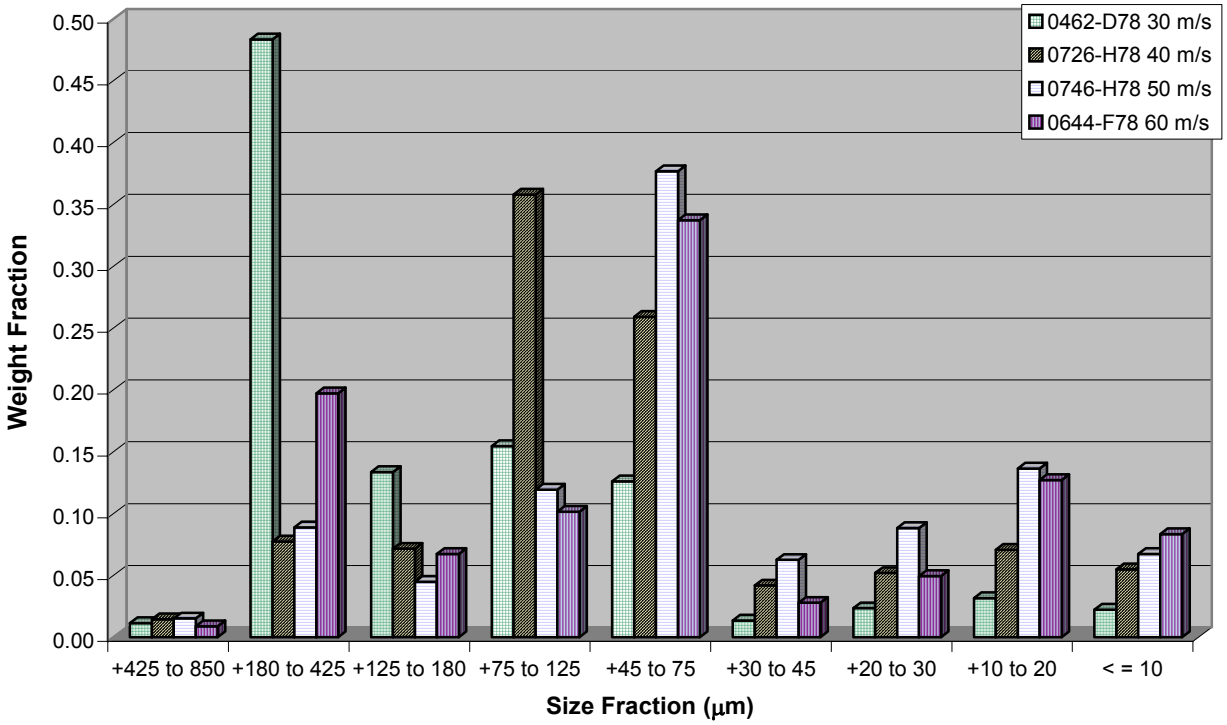

Figure 10. Impacted Heat Source Size Fractions

Table 5 Impacted Heat Source Size Fractions

	Weight Fraction			
Particle Size	0462-D78	0726-H78	0746-H78	0644-F78
(micron)	30 m/s	40 m/s	50 m/s	60 m/s
+425 to 850	0.0115	0.0145	0.0152	0.0088
+180 to 425	0.4833	0.0774	0.0888	0.1973
+125 to 180	0.1336	0.0716	0.0449	0.0674
+75 to 125	0.1545	0.3578	0.1194	0.1016
+45 to 75	0.1260	0.2591	0.3768	0.3371
+30 to 45	0.0136	0.0419	0.0626	0.0279
+20 to 30	0.0235	0.0520	0.0884	0.0495
+10 to 20	0.0316	0.0708	0.1365	0.1271
+9 to 10	0.0028	0.0059	0.0078	0.0098
+8 to 9	0.0025	0.0047	0.0067	0.0099
+7 to 8	0.0023	0.0032	0.0067	0.0069
+6 to 7	0.0023	0.0040	0.0060	0.0076
+5 to 6	0.0022	0.0032	0.0073	0.0075
+4 to 5	0.0025	0.0050	0.0069	0.0094
+3 to 4	0.0027	0.0085	0.0117	0.0128
+2 to 3	0.0017	0.0066	0.0057	0.0075
+1 to 2	0.0034	0.0138	0.0086	0.0119
<1	0.0000	0.0000	0.0000	0.0000

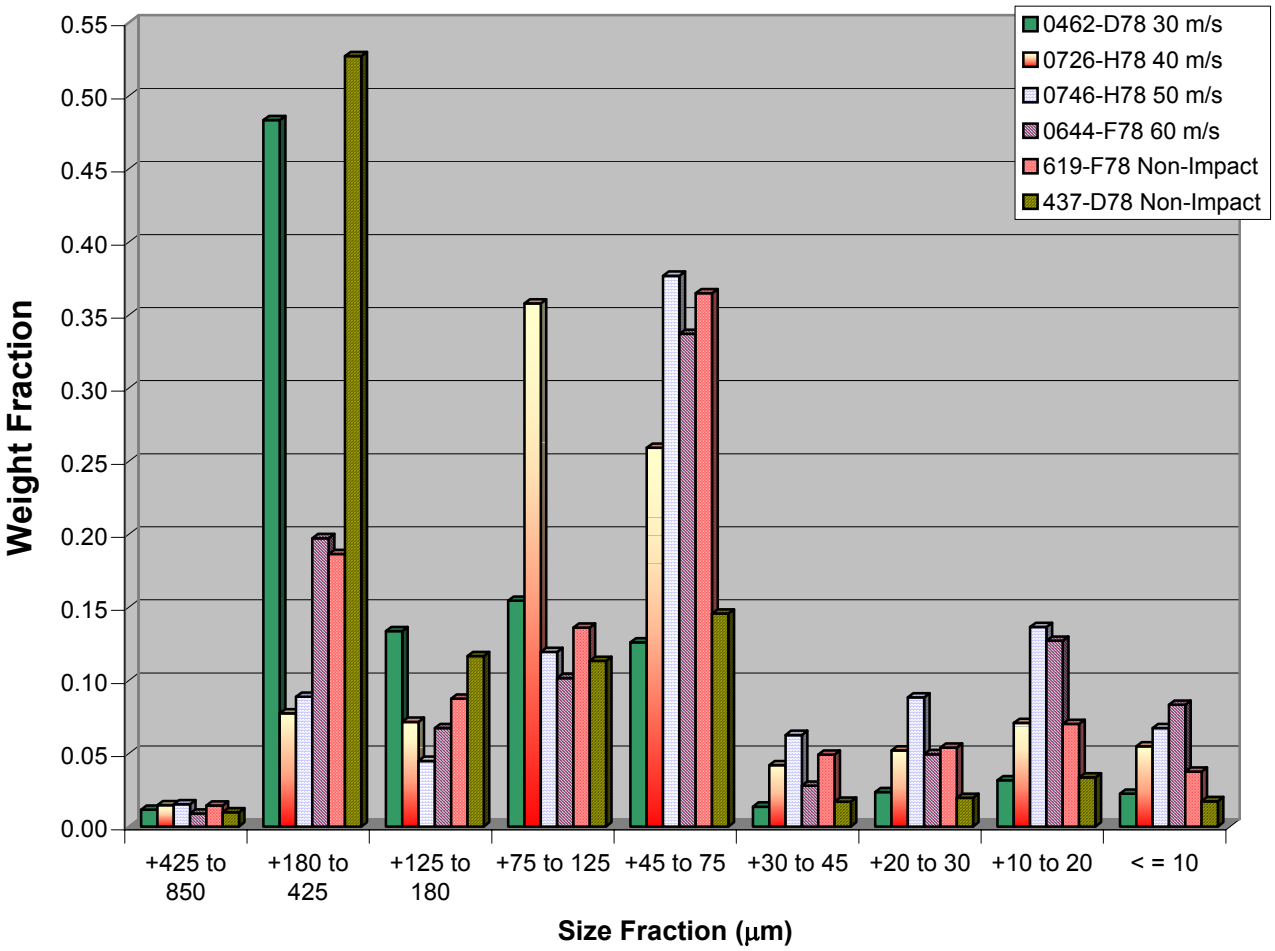

Figure 11. Combined Non-Impact and Impact Size Distribution

Table 6 shows particle size data for non-impacted and impacted heat sources. Included in this table is the historical average and historical one standard deviation for each size fraction. Not all size fractions are displayed due to the limited size fractions available for comparison from the historical data[1-5]. Figure 12 presents these data in graphical form.

Table 6 Particle Size Historical Statistical Comparison

		Weight (g)			
		< 20	10 to 20	5 to 10	<5
Non-Impact	MAD-619-F78	1.132	0.070	0.153	0.241
Non-Impact	MAD-437-D78	0.467	0.034	0.084	0.074
30 m/s	MAD-0462-D78	0.517	0.032	0.116	0.099
40 m/s	MAD-0726-H78	1.300	0.071	0.217	0.351
50 m/s	MAD-0746-H78	1.998	0.137	0.338	0.322
60 m/s	MAD-0644-F78	2.154	0.127	0.427	0.426
Non-Impact	Historical Ave	0.275	0.117	0.096	0.062
Non-Impact	Historical 1STD	0.173	0.078	0.058	0.048

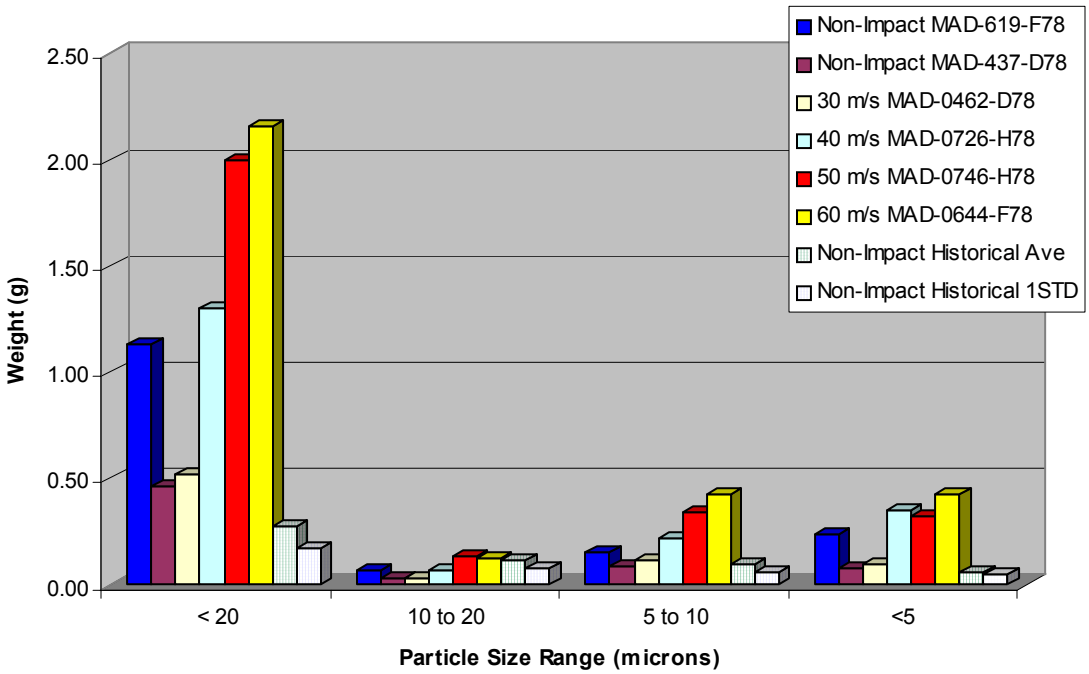

Figure 12. Particle Size Historical Statistical comparison

CONCLUSIONS

The fuel fragmentation response of fuel recovered from non-impact heat source 619-F78 was significantly different from the other non-impacted heat sources. It is possible that the particle size distribution of 619-F78 was due to the operating environment encountered during service. However, this hypothesis cannot be tested because the operating environment of this capsule is unknown. Particle size distribution of fuel recovered from non-impacted heat source 437-D78 was very similar to the historical non-impact data available, indicating that aging has a minimal effect on fuel fragmentation. However, a larger data sample would need to be evaluated to increase statistical confidence.

None of the impacted heat source capsules breached due to the impact event. There appears to be a correlation between fines generation particularly for the size fraction < 10 microns and impact velocity/ capsule deformation. The increase in fines generation for the size fraction § 10 microns of the impacted heat sources was small when compared to the non-impacted heat sources.

APPENDIX A

MILLIWATT FUEL PROCESSING FLOW DIAGRAM [6]

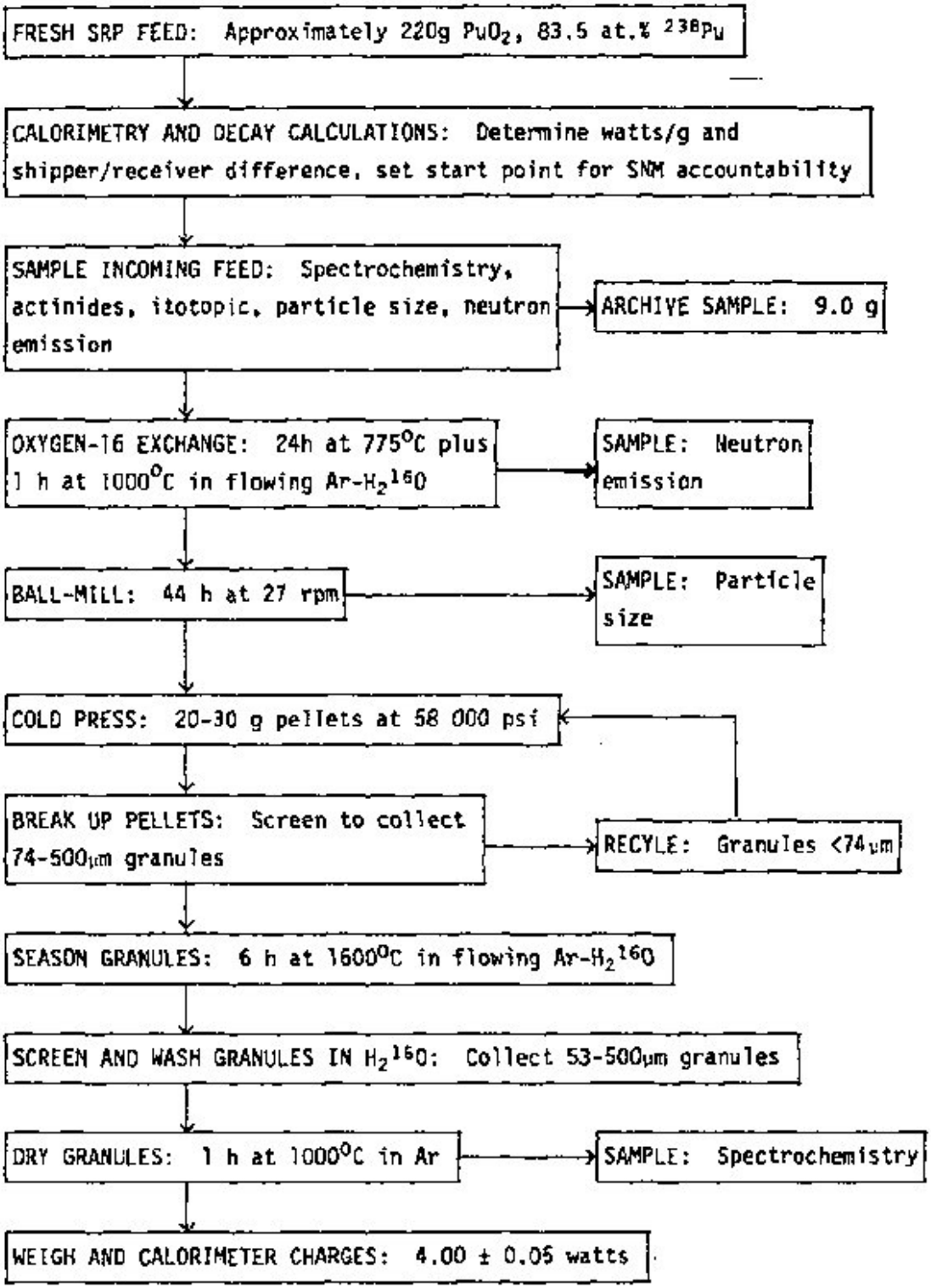

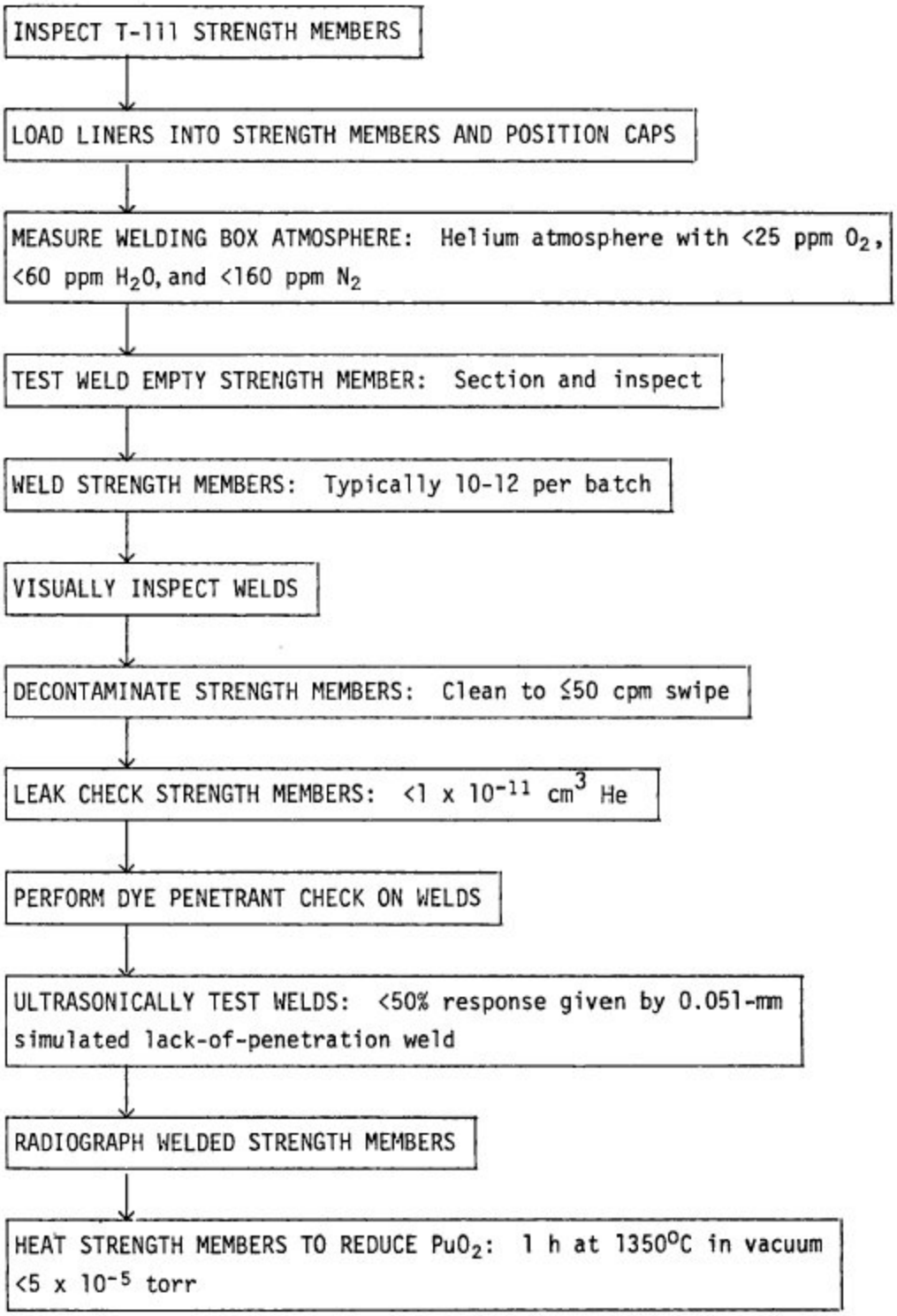
INSPECT T-111 STRENGTH MEMBERS
LOAD LINERS INTO STRENGTH MEMBERS AND POSITION CAPS
MEASURE WELDING BOX ATMOSPHERE: Helium atmosphere with <25 ppm O_2, <60 ppm H_2O, and <160 ppm N_2
TEST WELD EMPTY STRENGTH MEMBER: Section and inspect
WELD STRENGTH MEMBERS: Typically 10-12 per batch
VISUALLY INSPECT WELDS
DECONTAMINATE STRENGTH MEMBERS: Clean to ≤50 cpm swipe
LEAK CHECK STRENGTH MEMBERS: <1 x 10^{-11} cm^3 He
PERFORM DYE PENETRANT CHECK ON WELDS
ULTRASONICALLY TEST WELDS: <50% response given by 0.051-mm simulated lack-of-penetration weld
RADIOGRAPH WELDED STRENGTH MEMBERS
HEAT STRENGTH MEMBERS TO REDUCE PuO_2: 1 h at 1350°C in vacuum <5 x 10^{-5} torr

APPENDIX B

OVERALL MILLIWATT CAPSULE DIMENSIONS

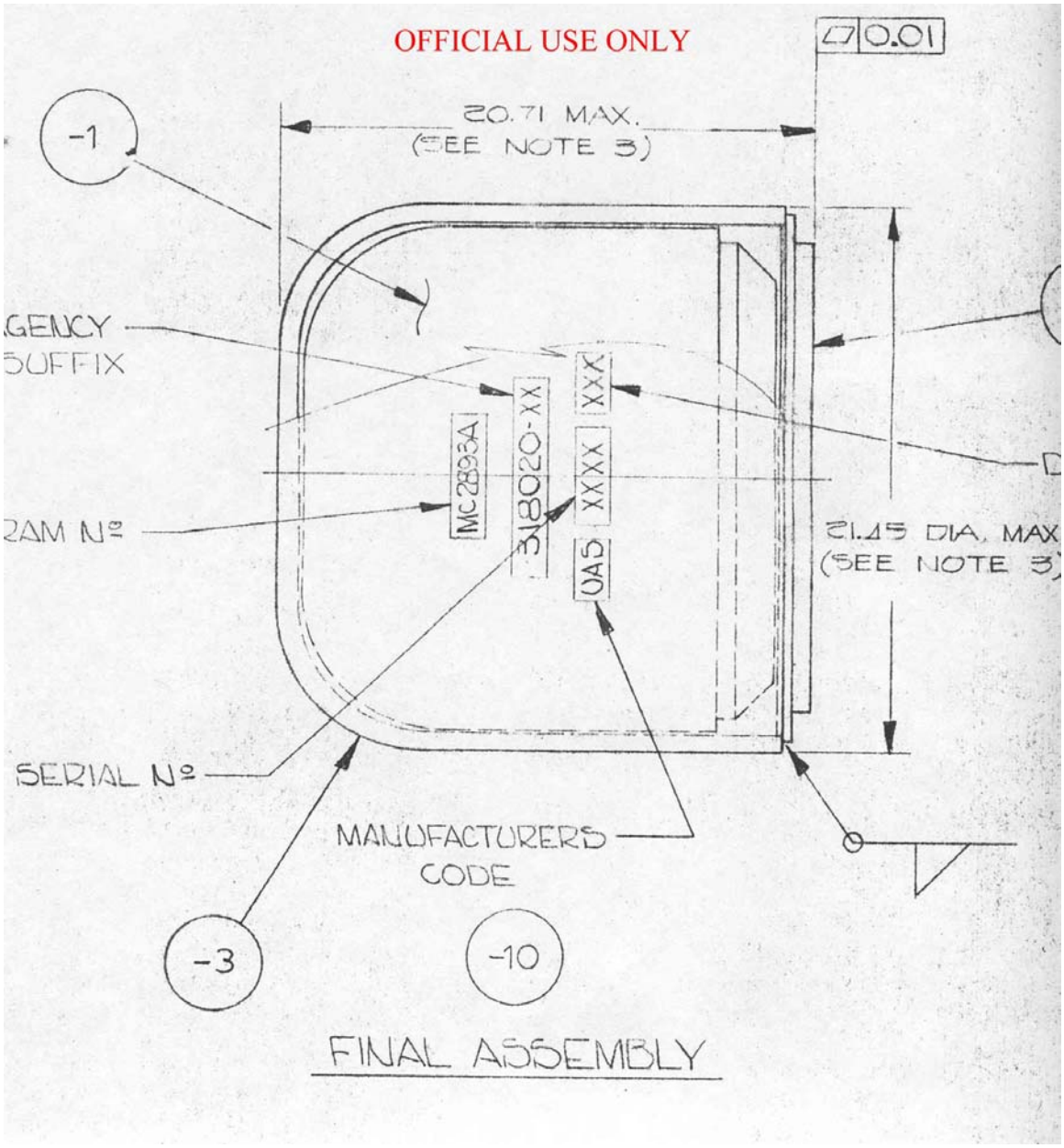

REFERENCES

1. G.H. Rinehart, T.W. Latimer, " Milliwatt Generator Project April 1983-March 1984",Los Alamos National Laboratory report LA-11220-PR
2. G.H. Rinehart, T.W. Latimer, " Milliwatt Generator Project April 1984-March 1986", Los Alamos National Laboratory report LA-11346-PR
3. G.H. Rinehart, T.W. Latimer, " Milliwatt Generator Project April 1986-March 1988", Los Alamos National Laboratory report LA-12236-PR
4. T.W. Latimer, "Milliwatt Generator Project April 1988-Sept 1986", Los Alamos National Laboratory report LA-13258-PR
5. G.H. Rinehart, T.W. Latimer, " Milliwatt Generator Project April 1982-March 1983", Los Alamos National Laboratory report LA-11217-PR
6. R.A. Kent, C.E. Frantz, C.C. Land, T.H. Feiertig, G.H. Rinehart, W.A. Stark, “Milliwatt Generator Project October 1980 – March 1981”, Los Alamos National Laboratory report LA-8881-PR